

8. B. Ha, N. V. Hieu, and N. Hoai (2005), “*Lectures on electron structures of graphene and graphene bilayer*,” Advanced Center of Physics Vietnam Academy of Science and Technology, pp. 1–4.
9. T. Ando (2007), “Magnetic oscillation of optical phonon in graphene”, *J. Phys. Soc. Jpn*, Vol. 76, No. 2, p. 024712.
10. A. K. Geim and K. S. Novoselov (2007), “The rise of graphene, *Nature Materials*”, Vol. 6, No. 3, pp. 183–191.
11. V.T. Truong, P. J. McMahon and A. R. Wilson (2012), *J. Polym. Sci. Part B: Polym. Phys.*, Vol.50, p. 624.
12. P. Avouris and F. Xia (2012), *MRS Bulletin*, Vol. 27, p.1225.

ẢNH HƯỞNG CỦA KÍCH THƯỚC GRAPHENE LÊN HỆ SỐ HẤP THỤ SÓNG ĐIỆN TỪ YẾU TRONG GRAPHENE HAI CHIỀU

Tóm tắt: Trên cơ sở phương trình động học lượng tử đã nhận được biểu thức giải tích cho mật độ dòng điện và hệ số hấp thụ sóng điện từ trong graphene hai chiều (2D graphene) với giả thiết tán xạ electron - phonon quang là trội. Sự phụ thuộc của hệ số hấp thụ vào các tham số đặc trưng cho trường ngoài và các tham số kích thước của graphene là rất phức tạp và phi tuyến. Các kết quả được tính toán và vẽ đồ thị đã minh chứng tốt cho các kết quả lý thuyết. Các kết quả được so sánh với trường hợp trong chất bán dẫn khối cho thấy sự khác biệt và tính mới của kết quả.

Từ khóa: Hệ số hấp thụ, phương trình động học lượng tử, 2D Graphene.

ORIGINAL ARTICLE CHARACTERISTIC INVESTIGATIONS OF A COMMERCIAL CYLINDRICAL-TYPE LITHIUM-ION BATTERY

Nguyen Van Nghia, Nguyen Van Ky, Luong Trung Son, Nguyen Thi Thu Hoa,
Hoang Manh Ha, Nguyen Si Hieu, Ta Anh Tan, Dang Tran Chien

*Hanoi Architectural University, Hanoi Architectural University,
Le Quy Don Technical University, Vietnam Academy of Science and Technology, Hanoi
Metropolitan University, Hanoi University of Natural Resources and Environment*

Abstract: *A commercial 4000 mAh cylindrical 26650-type lithium-ion battery was disassembled for the purpose of studying the electrode materials that defines the electrochemical performance of the battery. The cathode material is found to be a mixture of LiM_2O_4 and LiMO_2 oxides ($M = \text{Mn, Co, Ni, Al}$ or its combinations) and the anode material is dominated by graphite. The cathode materials composes of the homogeneous particles with mean diameter of 1 to 3 μm meanwhile the mean diameter of the graphite particles is about 10 μm . The first discharge capacity of the battery is 3820 mAh, which accounted for approximately 95.5% of the nominated capacity. The discharge capacity is gradually decreases during cycling. The average discharge voltage plateau is approximately 3.7 V, which is identical with the rated working voltage battery.*

Keywords: *Lithium-ion battery, commercial battery, anode materials, cathode materials, lithium compounds.*

Received: 25 March 2020

Accepted for publication: 20 April 2020

Email: dtchien@hunre.edu.vn

1. INTRODUCTION

Lithium-ion batteries (LIBs) have attracted much attention in the past few decades. Due to high energy density, reduced pollution, stable performance and long-life cycle, the commercial lithium-ion batteries are widely used to supply power for electric vehicles (EVs), electronic devices and battery energy storage (BES) for renewable energy [1]. Lithium-ion batteries have been widely used in portable electronic products and transportation vehicles. The lithium-ion battery has multiple sub-types such as the aqueous lithium-ion battery, nickel manganese cobalt oxide battery, and lithium-ion phosphate battery [2].

According to a research from Frost & Sullivan, the global lithium-ion battery market is expected to be worth \$22.5 billion in 2016. North America and China hold more than half the global revenues for LiBs. The global lithium-ion market size was around \$35 billion to \$40 billion as of 2018, and the demand will be incrementing at a positive Compound Annual Growth Rate (CAGR) of 13% to 18% during the forecast period of 2019 to 2025 [2]. In general, battery applications are predicted to have a turnover of \$90 billion by 2025. Investments of five companies such as Siemens, Total, Daimler, Dyson, AshiKasei, Catl, Tesla/Panasonic are over 13.7 billion USD that have been spent or planned in 2016 and 2017. In there, Contemporary Amperex Technology Co Ltd. (CATL) accounted for \$2.9 billion [3]. There are many lithium ion battery manufacturers in China. Those factories are separated in two kinds. One is the packaging factory which buys the battery cell and assembles the battery packs including mobile battery, laptop battery, storage battery, RC battery. Some of these kinds are Desay Battery Technology, Sunwoda Electronic, Eve Energy manufactures that do battery packaging for Huawei Technologies and Apple Inc.

According to a study of Jeff Desjardins [4], global lithium-ion battery production capacity will increase by 521% between 2016 and 2020. The capacity in 2016 was 28 GWh, and it will reach 174 GWh in 2020. By 2020, mass production of lithium batteries will still be dominated by 4 countries including USA, Poland, Korea and China. The lithium-ion battery capacity of China will rise to 62% (108 GWh) by 2020.

Although lithium batteries were commercialized in 1991 by Sony [5,6], scientists have been constantly researching to improve the performance of batteries and reduce the product's costs. The studies were mainly focused on the materials used to fabricate the cathodes, anodes and electrolytes of the batteries. In addition, numerous investigations have been paid on the overcharge/over-discharge failure [1], cycle aging at different temperatures [7], potential dependence of gas evolution in 18650 cylindrical cells [8], the impedance characteristics at various conditions [9], working at very high temperature for capacity fading and understanding of aging mechanisms [10], analyzing the rechargeable LiBs after prolonged cycling [11], interfacing investigations of a commercial lithium ion battery graphite anode material [12], etc. In this work, a commercial lithium-ion battery was investigated.

2. CONTENT

2.1. Materials and Methods

A 26650 cylindrical Li-ion battery was dismantled in a box filled with argon to separate the cathode tape and anode tape. The anode and cathode materials were easily collected from the electrode tapes. The crystal structure of the electrode materials was identified by X-ray diffraction (XRD, D8 Advance Bruker, Cu K α radiation, $\lambda = 1.5406 \text{ \AA}$). The XRD data were collected in the diffraction angle range (2θ) between 10° and 70° . The morphologies of the materials were observed using scanning electron microscopy (SEM, Jeol 6490 JED 2300,

Japan). The charge/discharge measurements were taken using an Auto-Lab Potentiostat PGS-30. All cells were cycled between 3.0 - 4.25 V at current density of 0.2 C.

2.2. Results and Discussion

A conventional LiB usually consists of two electrodes (a negative and a positive electrode), an electrolyte, and a porous polymer separator. The positive electrode was made of a transition metal oxide or a phosphate, while the negative was made of graphite. The electrolyte most often composed of an organic solvent containing a lithium salt. The porous polymer separator separated the two electrodes and prevents them from short circuit. The electrolyte easily penetrates into the porous polymer separator. During charging, the electrons are made to be released at the cathode and move externally to the anode. At the same time, the lithium ions move in the same direction, but internally, from cathode to anode via the electrolyte. When the battery is discharged, electrons travel from anode to the cathode through the external load. Concurrently, lithium ions travel from anode to the cathode in the electrolyte.

In order to study on the cathode and anode materials, it is necessary to disassemble the battery and analyze the relevant battery components. The cutting positions are about 2 mm near the positive or negative connector. The procedure of the disassemble process is illustrated in Fig. 1.

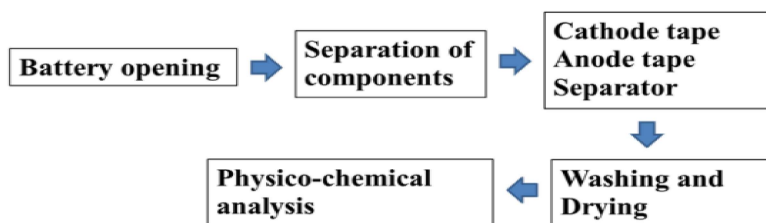


Fig.1. Chart for disassembling of the Li-ion battery.

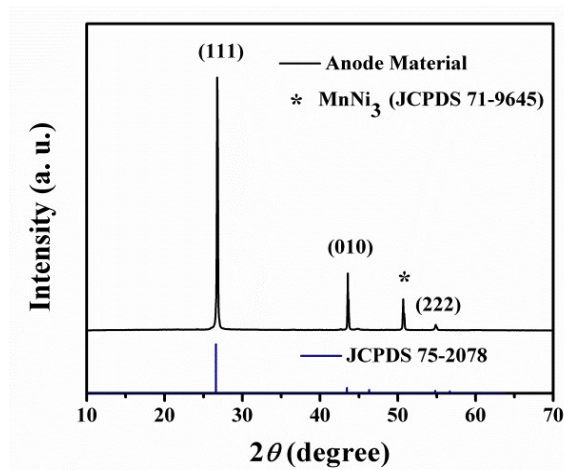


Fig. 2. XRD pattern of the anode of the battery

The XRD pattern of the anode material is shown in Fig. 2. Looking at the pattern, one can see that graphite dominated the field of anode materials of the battery. This phenomenon is due to graphite's competent capability of insertion and extraction of Li-ions. The diffraction peaks at the 2θ values of approximately 26.59° , 43.58° , 54.80° correspond to the (111), (010), (222) planes, respectively (JCPDS card No. 75-2078). One diffraction peak presented at the 2θ value of 50.70° is attributed to the MnNi_3 phase according to JCPDS card No. 71-9645. The MnNi_3 phase possibly formed due to the dissolve of Mn and Ni from the cathode material into the electrolyte then deposited onto the anode surface.

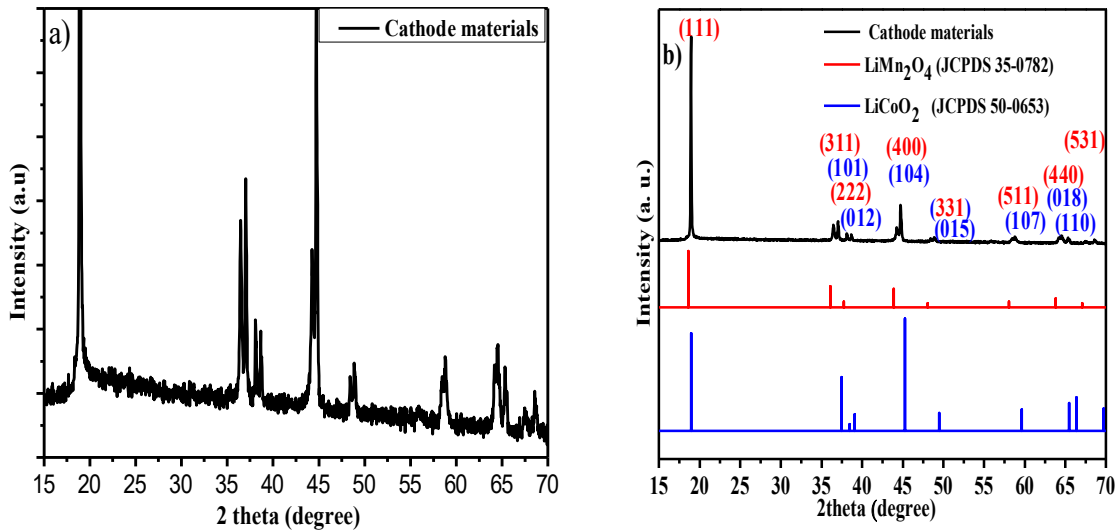


Fig. 3. (a) XRD pattern of the materials on cathode of the battery; (b) XRD pattern of the materials in compare with JCPDS 35-0782 and JCPDS 50-0653.

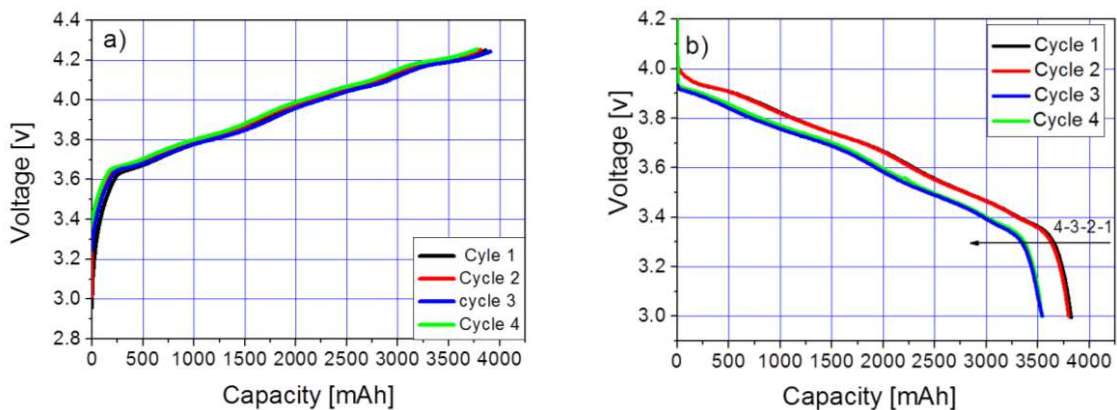


Fig. 4. (a) The first to the fourth charge cycle profiles and (b) discharge cycle profiles.

Figure 3a shows the XRD pattern of the materials on the battery cathode. To recognize what are the structures of the materials, the XRD pattern of the materials is put in the same graph with two JCPDS 35-0782 (LiMn_2O_4) and JCPDS 50-0653 (LiCoO_2) cards in Fig. 3b.

The results show that the cathode compounds have two structures, one is the spinel structure which is identical with the structure of the LiMn_2O_4 oxide and another one is P2 layer structure which is the same with the structure of the LiCoO_2 oxide.

Figure 4a and Fig. 4b show the battery voltage versus capacity during the charging and discharging processes at current density of 0.2 C between 3.0 - 4.25 V. The charge curves are similar and almost overlap which means the Li^+ ions can insert into the electrode materials reversibly (Fig. 4a). The discharge curves have the same shape which means the Li^+ can extract from the electrode reversibly (Fig. 4b). The average charge voltage plateau and discharge plateau are appropriate 4.0 V and 3.7 V, respectively. The difference between charge voltage plateau and discharge voltage plateau is about 0.25 V suggested that the delithiation and the lithiation processes have a slightly polarization.

The charge capacities, discharge capacities and the corresponding coulomb efficiencies, which are the ratios of discharge capacities and charge capacities, of the first to the fourth cycles are listed in Table 1. It can be seen that the discharge capacities are gradually decreased and the Coulombic efficiencies are over 90%. The decrease of the discharge capacity *is assigned to* the formation of the solid-electrolyte interface layer during the initial lithiation, which forms a barrier to the flow of lithium ions through the electrode [13]. This reduces the access to the active material.

Table 1. The charge and discharge capacities and coulomb efficiencies of the first to the fourth cycles

Cycle number	Charge capacity (mAh)	Discharge capacity (mAh)	Coulomb efficiency (%)
1	3863	3820	98.89
2	3809	3796	99.65
3	3911	3542	90.57
4	3778	3523	93.25

Table 2. Chemical components (wt%) of the anode at different zones

Zone	1	2	3
C	77.04	75.44	76.49
O	17.64	17.93	17.68
F	3.87	4.75	4.49
Si		0.17	
P	1.09	1.47	1.2
S	0.15	0.07	0.04
Ca			0.03
Fe	0.21	0.18	0.07

Total	100	100	100
-------	-----	-----	-----

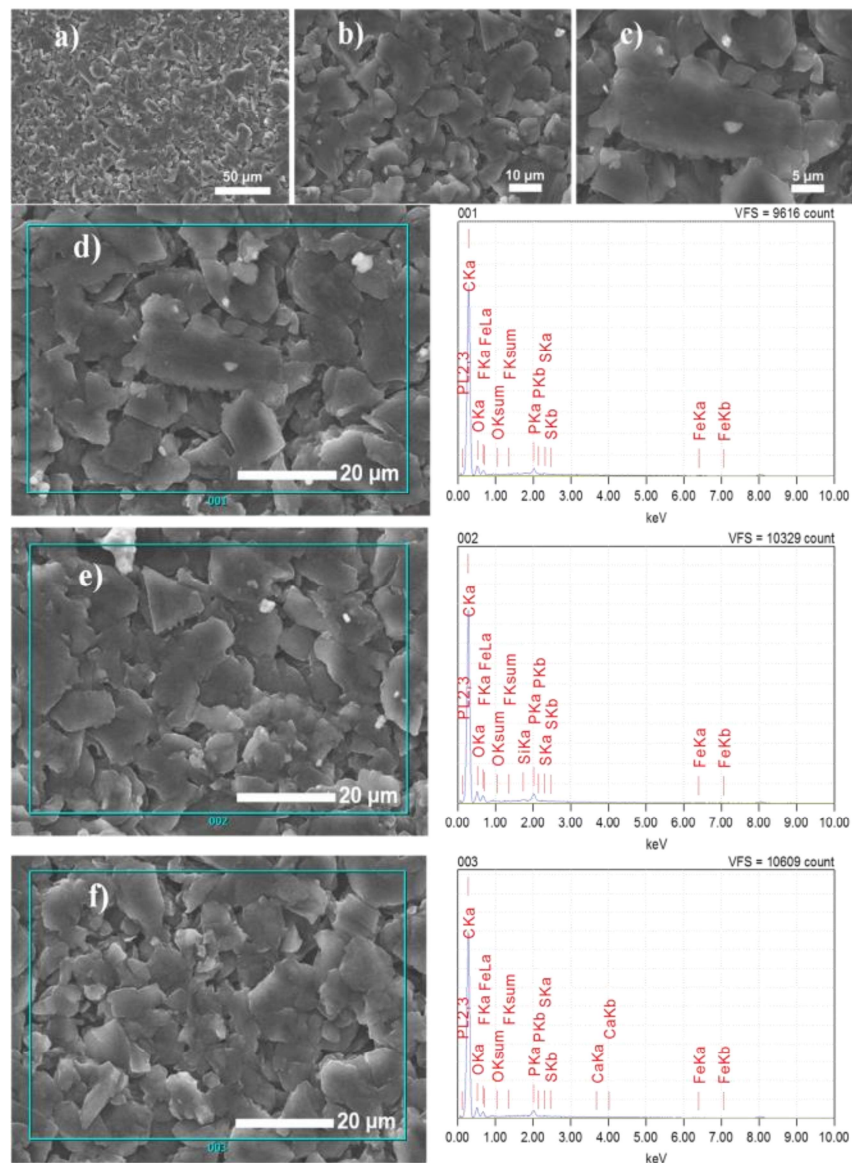


Fig. 5. (a, b, c) SEM images of anode of the battery; (d, e, f) EDS analysis result at 3 zones for anode of the battery

Figure 5a, 5b, 5c show the SEM images of the material that the anode of the battery is made of at different magnifications. Figure 5d, 5e, 5f show EDS analysis result at different zones of the anode. Table 1 reports the chemical analysis of the anode of the battery. As can be seen from Table 2, no other elements were detected in amount much higher than 1% but C, O, F. They are the main components in the anode in all three zones (C, O, F about 77%, 17%, 4%, respectively). Fe, P, S are presented in the anode with a very small in proportion. Especially, no Si and Ca were detected in zone 1, 3 and zone 1, 2, respectively.

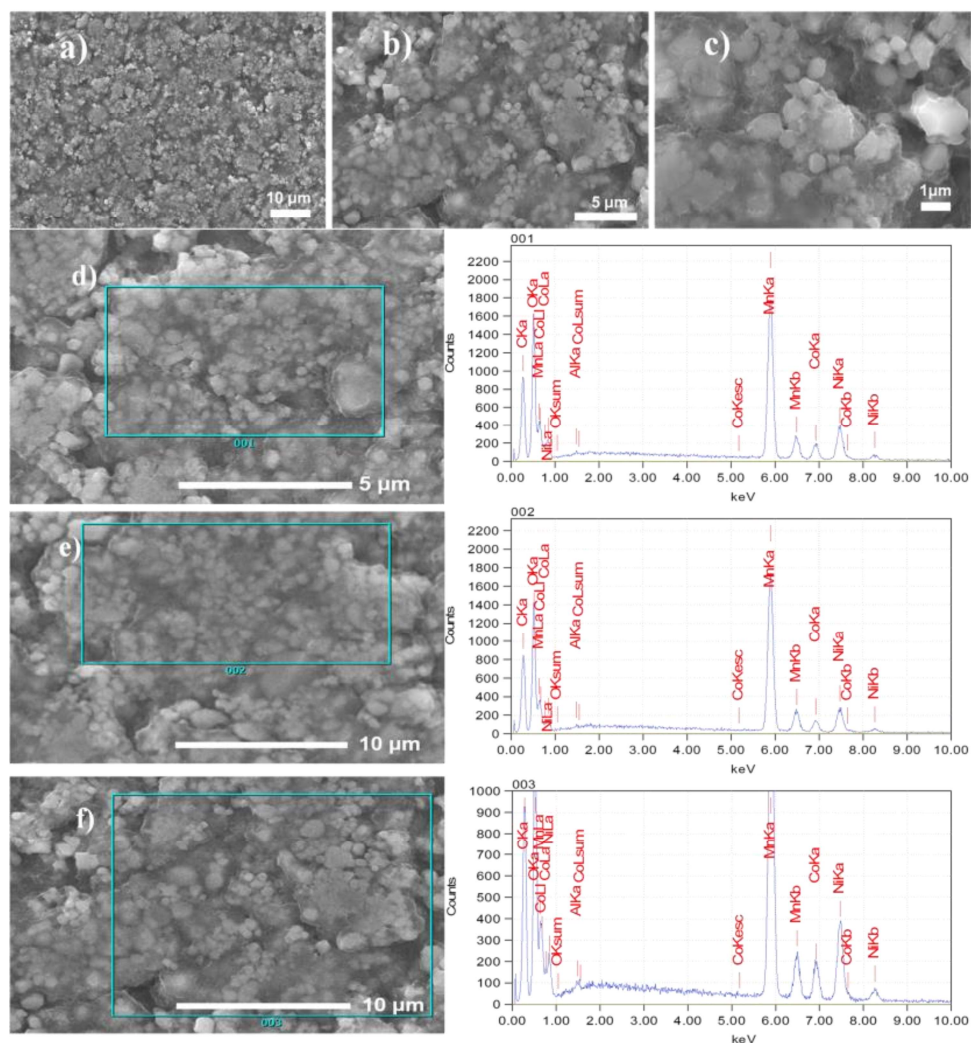


Fig. 6. (a, b, c) SEM images of the cathode; (d, e, f) EDS analysis result at 3 zones of the cathode.

Figure 6a, 6b, 6c show the SEM images of the material on the anode of the battery at different magnifications. Figure 6d, 6e, 6f show EDS analysis results at different zones of the cathode. Chemical analyses of the materials on the cathode are summarized in Table 3.

Table 3. Chemical components (wt%) of the cathode at different zones

Zone	1	2	3
C	22.96	22.71	24.67
O	24.27	24.51	23.35
Al	0.14	0.22	0.23
Mn	34.72	37.89	32.21
Co	5.12	4.28	5.6
Ni	12.78	10.41	13.94

Total	100	100	100
-------	-----	-----	-----

As can be seen from Table 3, Al element was detected in amount much smaller than 1%. The Mn, Co, Ni - transition metals present at about 34%, 5% and 12%, respectively, suggesting the presence of several lithium compounds that contain transition metal oxides (Mn, Co, Ni).

3. CONCLUSION

A commercial lithium-ion battery was disassembled to investigate. The characterization has been carried out by analysis means using EDS, XRD and SEM after having dismantled the battery into the single components. The results show that the anode is dominantly made of graphite while the cathode is made of LiM_2O_4 and LiMO_2 oxides ($M = \text{Mn, Ni, Co, Al}$ or its combinations). The charge and discharge profiles at current density of 0.2 C (800 mA), between 3.0 - 4.25 V show that the battery has the first discharge capacity of 3820 mAh and the capacity is gradually decreased during cycling. The average working voltage is about 3.7 V which is well consisted with the rated voltage released by the provided company.

Acknowledgements

This research is funded by Vietnam National Foundation for Science and Technology Development (NAFOSTED) under grant number 103.02-2018.22.

Notes: The authors declare no competing financial interest.

REFERENCES

1. D. Ouyang, M. Chen, J. Liu, R. Wei, J. Weng, J. Wang (2018), *Investigation of a commercial lithium-ion battery under overcharge/over-discharge failure conditions*, RSC Adv.8 33414-33424.
2. N. Imanishi, T. Horiuchi, A. Hirano, Y. Takeda (2001), *Lithium intercalation mechanism of iron cyanocomplex*, Studies in Surface Science and Catalysis 132 935-938.
3. H. Qiao, Q. Wei (2012), *Functional Nanofibers in Lithium-ion batteries*, in: Q. Wei (Eds.), *Functional Nanofibers and their Applications*, Woodhead Publishing Series in Textiles, Oxford, UK, pp. 197-208.
1. 7. K. Jalkanen, J. Karppinen, L. Skogstrom, T. Laurila, M. Nisula, K. Vuorilehto (2015), *Cycle aging of commercial NMC/graphite pouch cells at different temperatures*, Appl. Energy 154, p.160-172.
2. 8. B. Gerelt-Od, H. Kim, U. J. Lee, J. Kim, N. Kim, Y. J. Han, H. Son, S. Yoon (2018), *Potential Dependence of Gas Evolution in 18650 Cylindrical Lithium-Ion Batteries Using In-Situ Raman Spectroscopy*, J. Electrochem. Soc. 165 A168-A174.
10. W. Waag, S. Käbitz, D. U. Sauer (2013), *Experimental investigation of the lithium-ion battery impedance characteristic at various conditions and aging states and its influence on the application*, Appl. Energy 102 885-897.
11. L. Bodenes, R. Naturel, H. Martinez, R. Dedryvere, M. Menetrier, L. Croguennec, J. Peres, C. Tessier, F. Fischer (2013), *Lithium secondary batteries working at very high temperature: Capacity fade and understanding of aging mechanisms*, J. of Power Sources 236 265-275.
12. D. Aurbach, B. Markovsky, A. Rodkin, M. Cojocar, E. Levi, H. Kim (2002), *An analysis of*